Exosome-based delivery of super-repressor IκBα ameliorates kidney ischemia-reperfusion injury

see commentary on page 508

Seonghun Kim[1,7], Sul A Lee[2,3,7], Heakyung Yoon[4], Myung Yoon Kim[4], Jae-Kwang Yoo[4], So-Hee Ahn[4], Cheol Hyoung Park[4], Jimin Park[5], Bo Young Nam[5], Jung Tak Park[2], Seung Hyeok Han[2], Shin-Wook Kang[2], Nam Hee Kim[1], Hyun Sil Kim[1], Dawool Han[1], Jong In Yook[1], Chulhee Choi[4,6] and Tae-Hyun Yoo[2]

[1]Department of Oral Pathology, Oral Cancer Research Institute, College of Dentistry, Yonsei University, Seoul, South Korea; [2]Department of Internal Medicine, College of Medicine, Institute of Kidney Disease Research, Yonsei University, Seoul, South Korea; [3]Department of Internal Medicine, MetroWest Medical Center, Framingham, Massachusetts, USA; [4]ILIAS Innovation Center, ILIAS Biologics Inc., Daejeon, South Korea; [5]Severance Biomedical Science Institute, College of Medicine, Yonsei University, Seoul, South Korea; and [6]Department of Bio and Brain Engineering, Korea Advanced Institute of Science and Technology (KAIST), Daejeon, South Korea

Ischemia-reperfusion injury is a major cause of acute kidney injury. Recent studies on the pathophysiology of ischemia-reperfusion-induced acute kidney injury showed that immunologic responses significantly affect kidney ischemia-reperfusion injury and repair. Nuclear factor (NF)-κB signaling, which controls cytokine production and cell survival, is significantly involved in ischemia-reperfusion-induced acute kidney injury, and its inhibition can ameliorate ischemic acute kidney injury. Using EXPLOR, a novel, optogenetically engineered exosome technology, we successfully delivered the exosomal super-repressor inhibitor of NF-κB (Exo-srIκB) into B6 wild type mice before/after kidney ischemia-reperfusion surgery, and compared outcomes with those of a control exosome (Exo-Naïve)-injected group. Exo-srIκB treatment resulted in lower levels of serum blood urea nitrogen, creatinine, and neutrophil gelatinase-associated lipocalin in post-ischemic mice than in the Exo-Naïve treatment group. Systemic delivery of Exo-srIκB decreased NF-κB activity in post-ischemic kidneys and reduced apoptosis. Post-ischemic kidneys showed decreased gene expression of pro-inflammatory cytokines and adhesion molecules with Exo-srIκB treatment as compared with the control. Intravital imaging confirmed the uptake of exosomes in neutrophils and macrophages. Exo-srIκB treatment also significantly affected post-ischemic kidney immune cell populations, lowering neutrophil, monocyte/macrophage, and T cell frequencies than those in the control. Thus, modulation of NF-κB signaling through exosomal delivery can be used as a novel therapeutic method for ischemia-reperfusion-induced acute kidney injury.

Kidney International (2021) **100,** 570–584; https://doi.org/10.1016/j.kint.2021.04.039

KEYWORDS: acute kidney injury; apoptosis; exosome; inflammation; ischemia-reperfusion injury; NF-κB signaling

Copyright © 2021, International Society of Nephrology. Published by Elsevier Inc. All rights reserved.

Translational Statement

Despite the recent advancements in understanding of the pathophysiology of acute kidney injury (AKI), no drug with proven clinical efficacy and safety is available for AKI treatment. By using a novel optogenetically engineered exosome technology to deliver the exosomal super-repressor inhibitor of nuclear factor (NF)-κB (Exo-srIκB) into mice before or after kidney ischemia-reperfusion surgery, our study showed that the systemic delivery of Exo-srIκB alleviated renal damage in experimental ischemic AKI. This result suggests that modulating NF-κB signaling through exosomal delivery can be used as a novel therapeutic method for AKI. Our plan for future first-in-human study using Exo-srIκB in AKI will shed more light on its potential clinical applicability.

Ischemia-reperfusion (IR)–induced acute kidney injury (AKI) is a relatively common but severe medical condition that can happen with systemic hypoperfusion followed by restoration of blood flow and reoxygenation.[1] Renal IR injury (IRI) is associated with a high morbidity and mortality and is known to induce dysfunction in other distant organs, including the heart, lung, and liver.[2]

In IR-induced AKI, hypoxia and reperfusion generate reactive oxygen species, followed by a cascade response, including cell death and inflammation, and subsequent renal failure.[3] Recent advancements in understanding of the detailed mechanism of IR-induced AKI have highlighted the importance of immunologic responses in the course of renal IRI.[4–7]

Correspondence: *Tae-Hyun Yoo, Department of Internal Medicine, College of Medicine, Institute of Kidney Disease Research, Yonsei University, 50-1 Yonsei-ro, Sinchon-dong, Seodaemun-gu, Seoul, South Korea. E-mail: yoosy0316@yuhs.ac; or Jong In Yook, Department of Oral Pathology, Oral Cancer Research Institute, College of Dentistry, Yonsei University, 50-1 Yonsei-ro, Sinchon-dong, Seodaemun-gu, Seoul, South Korea. E-mail: jiyook@yuhs.ac; or Chulhee Choi, CEO and CSO, ILIAS Biologics Inc., 40-20, Techno 6-ro, Yuseong-gu, Daejeon 34014, South Korea or Department of Bio and Brain Engineering, KAIST, 291 Daehak-ro, Yuseong-gu, Daejeon 34141, South Korea. E-mail: cchoi@iliasbio.com*

[7]SK and SAL contributed equally to the manuscript.

Received 13 August 2020; revised 22 April 2021; accepted 30 April 2021; published online 27 May 2021

Nuclear factor (NF)-κB plays a pivotal role in ischemic AKI, and orchestrates the inflammatory response and cell survival.[8]

More than 800 synthetic and natural materials are known to be partly involved in modulating NF-κB activation.[9] Several studies have shown that NF-κB signaling blockades, such as the renin–angiotensin–aldosterone system blockade or tumor necrosis factor-α (TNF-α) blocker, can alleviate kidney damage.[10–12] However, their mechanisms of action are pleiotropic and lack specificity. Recent advancements in nanotechnology made it feasible to produce specific gene sequences or nanoparticles to target NF-κB signaling. These specific NF-κB inhibitors showed better renal outcomes in various types of experimental AKI models.[13–15] However, no NF-κB inhibitor has been commercially approved for human use yet.

Successful gene and drug delivery require the selection of an appropriate vector for delivering target molecules stably to the site of action, without causing adverse effects to the recipient. Various types of vectors, including recombinant adenoviruses, liposomes, ligand-conjugated nanoparticles, and ultrasound microbubbles, are reportedly efficient for drug delivery, because of their stability and high loading capacity.[16,17] However, they are rapidly recognized and cleared by the reticuloendothelial system, and their nonuniform particle size as well as their nonspecific uptake pattern limit their use as bio-carriers.[18] The high immunogenicity of adenoviral vectors and the potential hypersensitivity reactions of liposomes are additional limitations.[19,20]

Recently, exosomes received significant attention as novel biocarriers for gene and drug delivery. Exosomes are extracellular vesicles that play an important role in cell-to-cell communication, by transferring bioactive materials to recipient cells or affecting signaling pathways of target cells.[21] Exosomes are easier to store, and they exhibit greater stability.[22] Exosomes have a high capacity to overcome biological barriers, and they can carry surface molecules targeting specific cell types, thus causing fewer off-target effects.[23] However, in the clinical application of exosomes, it was a significant challenge to obtain high amounts of pure exosomes and load soluble proteins into exosomes. Using "exosomes for protein loading via optically reversible protein-protein interactions" (EXPLOR), a novel, optogenetically engineered exosome technology developed by Yim *et al.*, significant advancements in the production efficiency and biological compatibility of exosomes were achieved.[24] Briefly, EXPLOR technology induces the reversible conjugation between 2 photo-reactive binding proteins, CRY2 and CIBN, which are fused with either a cargo protein or an exosome marker by using blue-light illumination. This process results in the guidance of the cargo protein into the inner surface of the early endosomes and ultimately the secretion of cargo protein–carrying exosomes. These exosomes can be easily isolated and purified from the producing cell supernatant with blue-light removal, which allows the cargo protein to be present in free form in the luminal side of the exosomes. This EXPLOR technology has been adopted recently in the experimental sepsis model by Choi *et al.*; they administered exosomes containing the super-repressor IκB (srIκB) to mice.[25] This was a nondegradable form of kappa B inhibitor (IκB) that prevented the nuclear translocation of NF-κB. Their study showed that treatment with srIκB-containing exosomes (Exo-srIκB) ameliorated the systemic proinflammatory response and subsequent organ dysfunction in the mouse sepsis model.

In the present study, we used the same EXPLOR technology to load srIκB into exosomes and systemically deliver Exo-srIκB, to assess their effect on the course of ischemic AKI. Human embryonic kidney (HEK) 293T cell lines that produced 2 recombinant proteins, CIBN-EGFP-CD9 and srIκB-mCherry-CRY2, were used for producing Exo-srIκB, by inducing the transient docking of CRY2 and CIBN using blue-light illumination (Figure 1a). Control exosomes (Exo-Naïve) were generated from intact HEK293T cells. We aimed to examine whether optogenetically engineered Exo-srIκB could alleviate IR-induced kidney damage and whether it has a modulatory effect on inflammation and apoptosis.

METHODS

Animals

Most of the experiments used male C57BL/6J mice, which were bred under specific pathogen-free conditions at the central animal facility of the Yonsei Medical Center (Seoul, South Korea). An intravital imaging study was conducted using C57BL/6N mice at IVIM Technology (Daejeon, South Korea), due to a technical capacity issue. All experiments used male mice, aged 6–7 weeks. All animal procedures were performed in accordance with the Principles of Laboratory Animal Care (National Institutes of Health Publication no. 85-23, revised 1985) and were approved by the Institutional Animal Care and Use Committee (IACUC) at Yonsei University College of Medicine in Seoul, South Korea (IACUC Approval No. 2020-0060) and at IVIM Technology (IACUC Approval No. 2019-06.1).

Exosome isolation and characterization

The generation and isolation of Exo-srIκB have been thoroughly described previously.[24,25] The morphology of exosomes and the distribution of exosome particle numbers and sizes were confirmed by transmission electron microscopy and nanoparticle tracking analysis, respectively. Details of this process are provided in the Supplementary Methods.

Statistics

Data are expressed as means ± SD values. Statistical differences were analyzed using one-way analysis of variance with Bonferroni *post hoc* test for comparisons on more than 3 groups and the Mann-Whitney *U* test for nonparametric analysis between 2 groups using Prism 8 (GraphPad, San Diego, CA). Results were considered statistically significant when $P < 0.05$.

RESULTS

Characterization and analysis of engineered exosomes

The production, collection, and purification of exosomes have been thoroughly described in previous studies.[24,25] The size of particles mostly ranged from 30 to 120 nm, with a mean size of 101 nm. Transmission electron microscopy revealed intact cup-shaped membrane vesicles with sizes in accordance with nanoparticle tracking analysis results (Figure 1b and c). Immunoblotting analysis results for Exo-srIκB revealed the robust expression of target proteins, including srIκB, mCherry,

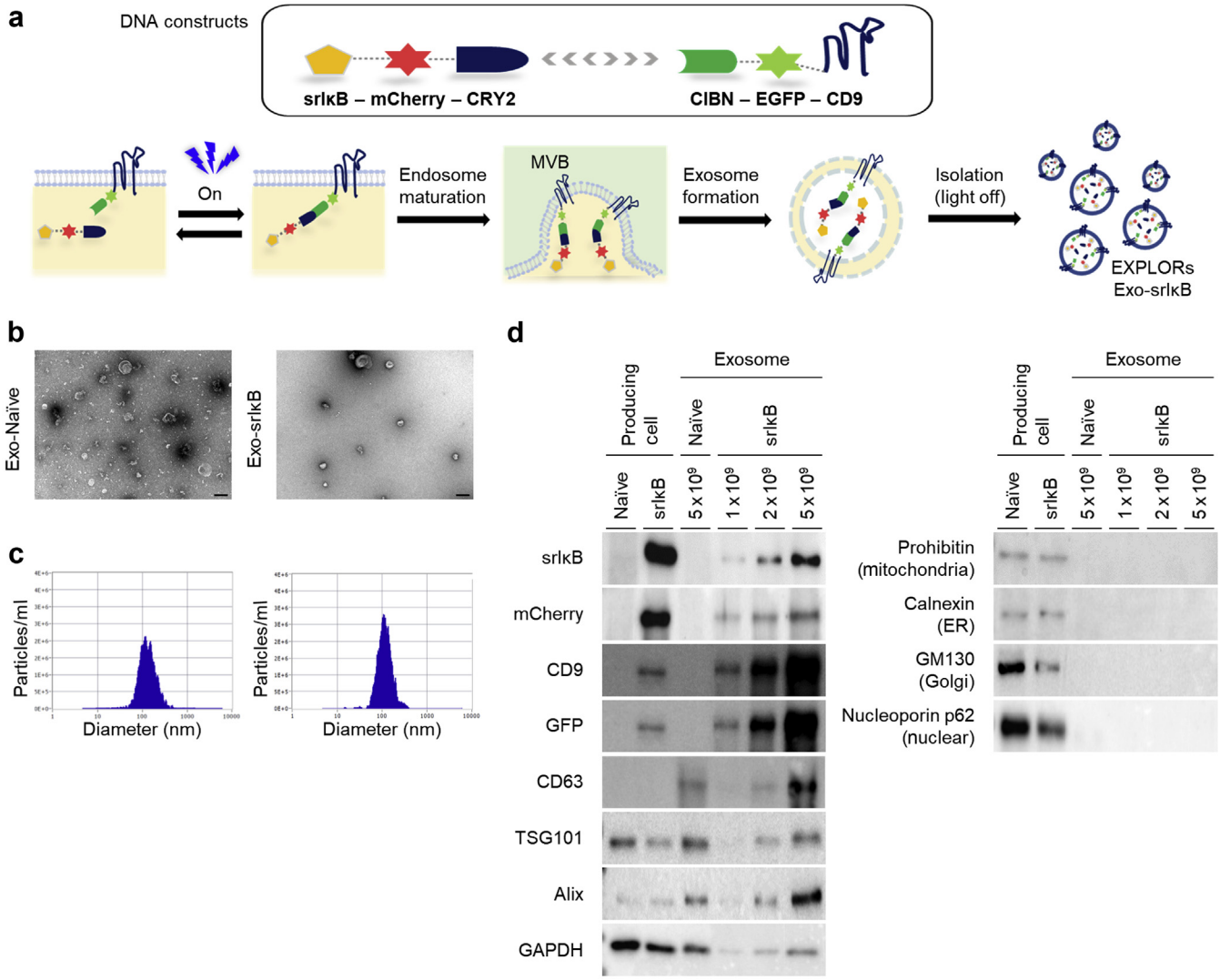

Figure 1 | Characterization of engineered exosomes produced from human embryonic kidney (HEK)293T. (**a**) Schematic diagram of DNA constructs used for producing super-repressor kappaB inhibitor (IκB)–loaded exosomes (Exo-srIκB) (upper), and biogenesis of cargo protein–carrying exosomes using optically reversible protein–protein interactions, so-called exosomes for protein loading via optically reversible protein-protein interactions (EXPLOR) technology (lower). (**b**) Representative transmission electron microscopy images of a control exosome (Exo-Naïve) and Exo-srIκB. Bar = 100 nm. (**c**) Concentrations and size distributions of Exo-Naïve (left) and Exo-srIκB (right) were determined by a Zetaview instrument (Particle Metrix, Germany). (**d**) Immunoblotting HEK293T cells and HEK293T cell–derived exosomes to analyze the expression of target proteins (srIκB, mCherry, CD9, and green fluorescent protein [GFP]), exosome-positive markers (CD63, TSG101, Alix, and glyceraldehyde-3-phosphate dehydrogenase [GAPDH]), and exosome-negative markers (cell organelle markers; prohibitin, calnexin, GM130, and nucleoporin p62). Naïve cells and Exo-Naïve cells were used as negative controls of Exo-srIκB. CIBN, N-terminal fragment of cryptochrom-interacting basic-helix-loop-helix 1; EGFP, enhanced green fluorescent protein.

CD9, and green fluorescent protein (GFP), with positive exosome markers, such as CD63, TSG101, Alix, and glyceraldehyde-3-phosphate dehydrogenase (GAPDH). Exo-srIκB lacked the expression of cell organelle markers, including prohibitin, calnexin, GM130, and nucleoporin p62. Exo-Naïve did not express any marker except exosome markers (Figure 1d).

Injection of Exo-srIκB ameliorates renal IRI

First, we investigated the role of Exo-srIκB in the course of renal IRI. Each experimental group was i.p. injected with 3×10^9 pn of Exo-srIκB or with Exo-Naïve 3 times in 1-hour intervals (total of 9×10^9 pn), either before or after renal IRI (pretreatment: 3, 2, and 1 hour before IRI surgery; post-treatment: 1, 2, and 3 hours after IRI surgery). This injection schedule was empirically determined to ensure delivery of exosomes to the target cells and tissues. Mice were sacrificed either 24 or 48 hours after surgery (Figure 2a).

Interestingly, the mouse group that received Exo-srIκB showed a significantly lower level of serum blood urea nitrogen and creatinine than the Exo-Naïve–injected group after IRI surgery, in both pretreatment and post-treatment models (blood urea nitrogen and creatinine at 24 hours and 48 hours in both models, $P < 0.001$; Figure 2b and c). Serum neutrophil gelatinase-associated lipocalin levels were significantly reduced

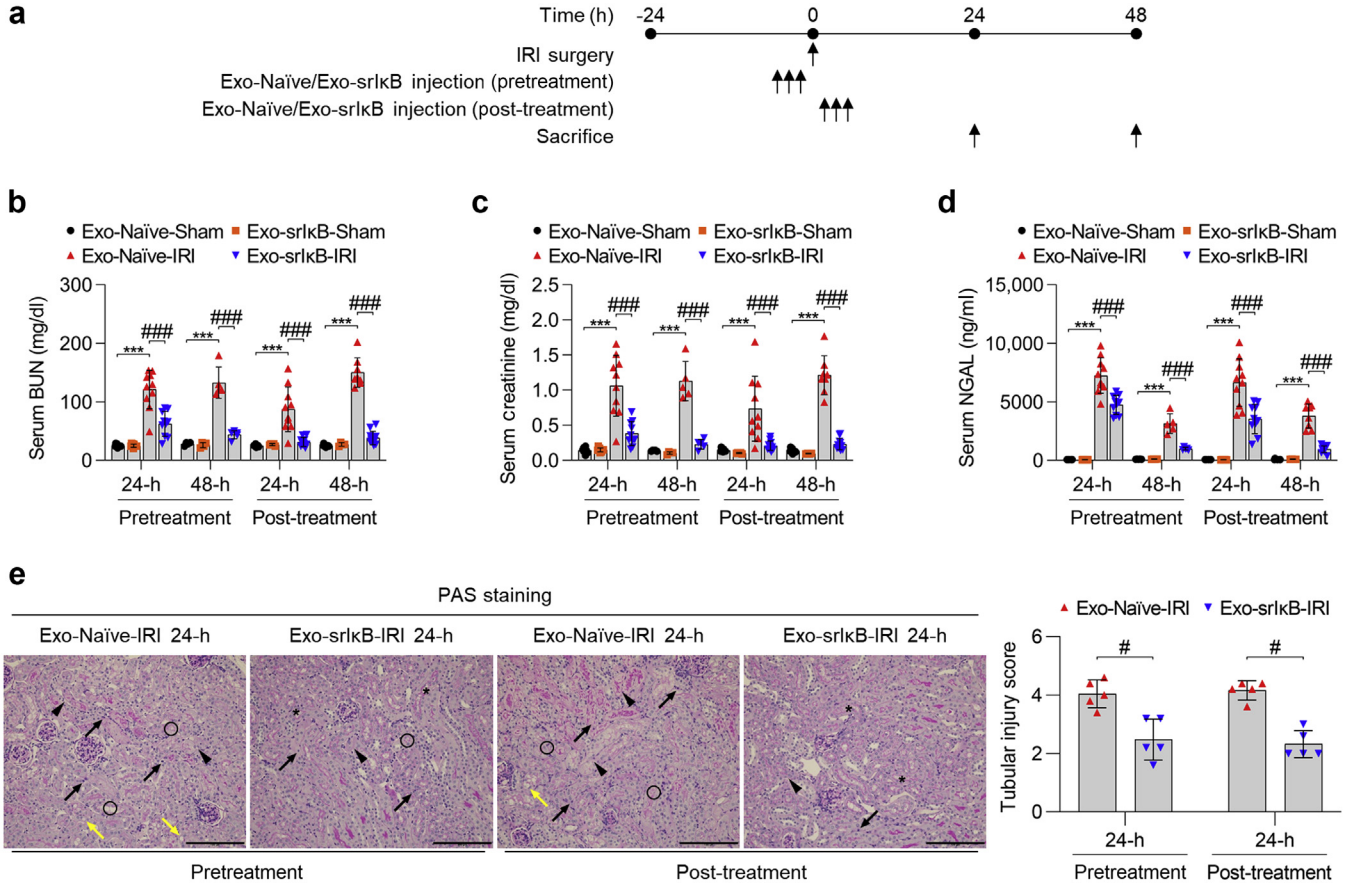

Figure 2 | Renal protective effects of super-repressor kappaB inhibitor–loaded exosomes (Exo-srIκB) after kidney ischemia–reperfusion injury (IRI). (**a**) Experimental scheme of kidney IRI surgery and exosome delivery. Each mouse group was i.p. injected with 3×10^9 pn of control exosomes (Exo-Naïve) or Exo-srIκB 3 times in a 1-hour (h) interval (total of 9×10^9 pn). Mice were killed either 24 hours (24-h) or 48 h (48-h) after IRI surgery, and serum and tissues were collected for further evaluation. (**b–d**) Serum levels of blood urea nitrogen (BUN), creatinine, and neutrophil gelatinase–associated lipocalin (NGAL) among different groups depending on treatment type (Exo-Naïve vs. Exo-srIκB), drug delivery timing (pretreatment vs. post-treatment), and follow-up time point (24-h and 48-h), which shows the renal protective effect of Exo-srIκB treatment (pretreatment 24-h, n = 10; pretreatment 48-h, n = 4–5; post-treatment 24-h, n = 5–10; post-treatment 48-h, n = 4–11). (**e**) (Left) Representative periodic acid–Schiff (PAS) staining images of cortical tubular cells in kidney sections from Exo-Naïve and Exo-srIκB treatment groups after renal IRI surgery. Normal proximal tubular brush border (*) or loss of brush border (o); chromatin condensation (black arrows); denuded basement membrane (black arrowheads); vacuolization (yellow arrows); bar = 100 μm. (Right) Pathologic tubular injury; kidney samples from each group show fewer tubular injuries with Exo-srIκB treatment than with Exo-Naïve treatment (pretreatment 24-h, n = 5; post-treatment 24-h, n = 5). Comparisons between groups were assessed using one-way analysis of variance with Bonferroni *post hoc* test and Mann-Whitney U test. Data are represented as mean ± SD values. $^{***}P < 0.001$ for comparison of the Exo-Naïve-Sham and Exo-Naïve-IRI surgery groups. $^{\#}P < 0.05$ and $^{\#\#\#}P < 0.001$ for comparison of the Exo-Naïve-IRI and Exo-srIκB-IRI surgery groups. To optimize viewing of this image, please see the online version of this article at www.kidney-international.org.

in the Exo-srIκB–injected group, compared with those in the Exo-Naïve group, in the pretreatment and post-treatment models ($P < 0.001$; Figure 2d). Histologic evaluation results also revealed lower tubular injury scores in the mouse group receiving the Exo-srIκB treatment, compared with those in the Exo-Naïve group, in the pretreatment and post-treatment models ($P < 0.05$ vs. Exo-Naïve–injected group; Figure 2e). Collectively, these data demonstrate that the systemic delivery of Exo-srIκB directly prevents the course of ischemic AKI.

Systemic Exo-srIκB treatment represses renal NF-κB signaling in IR-injured kidney

To understand the underlying mechanism by which systemic Exo-srIκB treatment affects the course of IR-induced AKI, we first checked whether the systemic delivery of Exo-srIκB represses local NF-κB signaling in kidneys. We measured the expression of NF-κB p65 protein in renal nuclear extracts from each different experimental group via Western blotting. Systemic treatment with 9×10^9 pn of Exo-srIκB significantly decreased IR-induced NF-κB nuclear translocation, compared with that in the Exo-Naïve–treated group, in the pre-IRI (24 hours after IRI, $P < 0.05$; 48 hours after IRI, $P < 0.001$) and post-IRI (24 and 48 hours after IRI, $P < 0.01$; Figure 3a) treatment models. We reconfirmed this finding by measuring the DNA binding activity of p65 using renal nuclear extracts from each experimental group. Exo-srIκB treatment significantly downregulated the DNA binding activity of NF-κB after kidney IRI, compared with that in the Exo-Naïve group,

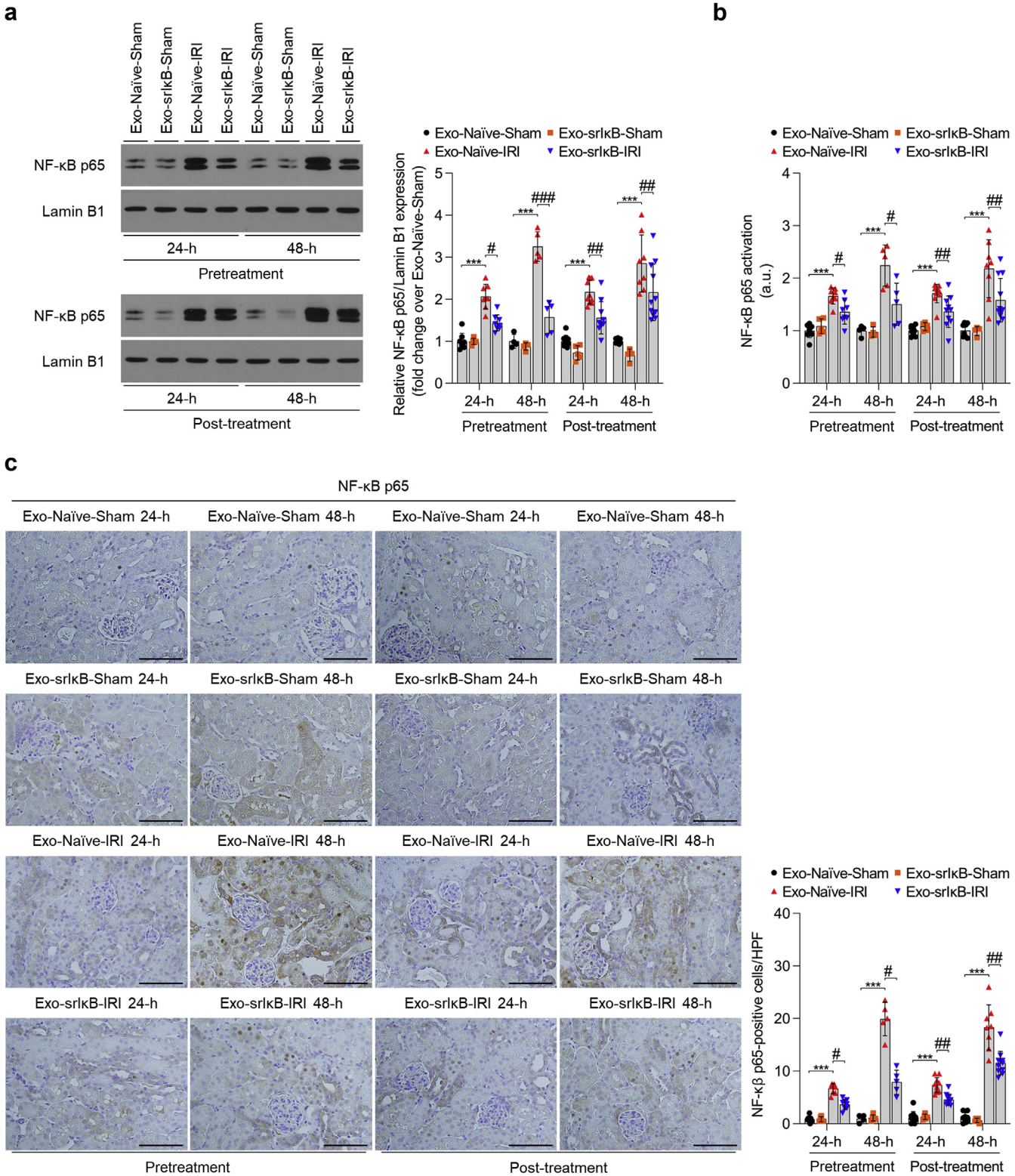

Figure 3 | Suppression of ischemia–reperfusion injury (IRI)–induced nuclear factor (NF)–κB activation following super-repressor kappaB inhibitor–loaded exosome (Exo-srIκB) treatment. (**a**) Western blot analysis of NF-κB p65 expression using renal nuclear extracts from each experimental mouse group. Nuclear extracts were biochemically separated from cytoplasmic fractions, and NF-κB p65 and Lamin B1 expression was analyzed via Western blotting. IRI-induced activation of NF-κB signaling was significantly repressed with perioperative Exo-srIκB treatment. (**b**) Elevated DNA-binding activity of NF-κB p65 following renal IRI was suppressed with perioperative Exo-srIκB treatment. (**c**) (Left) Representative immunohistochemical images with NF-κB p65 antibody from each treatment group. Bar = 50 μm. (Right) Graphical representation showing immunohistochemical detection of NF-κB p65 in each experimental group. Treatment with Exo-srIκB (continued)

regardless of treatment timings (pretreatment: 24 and 48 hours after IRI, $P < 0.05$; post-treatment: 24 and 48 hours after IRI, $P < 0.01$; Figure 3b). Further validation through NF-κB immunohistochemical staining showed a significant reduction in NF-κB expression in the Exo-srIκB–treated group, compared with that of the control treatment group (pretreatment: 24 and 48 hours after IRI, $P < 0.05$; post-treatment: 24 and 48 hours after IRI, $P < 0.01$; Figure 3c). Thus, systemic Exo-srIκB treatment can reduce renal NF-κB signaling in post-IR kidneys.

Exo-srIκB ameliorates inflammation in post-ischemic kidneys

To further investigate whether systemic exosomal srIκB treatment locally alleviates renal IRI-induced inflammation, we determined gene expression levels of pivotal inflammatory mediators, including *Il-1α*, *Il-1β*, *Il-2*, *Il-4*, *Il-6*, *Il-10*, *Il-17α*, *Ccl2*, *Ccl3*, *Ccl5*, *Cxcl2*, *Ifn-γ*, and *Tnf-α* through quantitative real-time polymerase chain reaction. Treatment with 9×10^9 pn of Exo-srIκB before IRI significantly suppressed the expression levels of *Il-1β*, *Il-6*, *Tnf- α*, *Ccl2*, *Ccl5*, and *Cxcl2*, compared with those of the Exo-Naïve–treated group in IR-injured kidneys (Figure 4a). Multiplex cytokine analysis was also performed using serum from different experimental groups. Results were less significant than kidney transcriptional data, but there was an obvious tendency for decreased expression of inflammatory cytokines, including IL-6, tumor necrosis factor–α, CCL2, CCL5, and CXCL2 in the Exo-srIκB treatment group, compared with that in the control group (Figure 4b).

Additionally, we evaluated the effect of exosomal srIκB treatment on the expression of adhesion molecules, by comparing transcriptomic and translational intercellular adhesion molecule 1 levels among treatment groups. Quantitative real-time polymerase chain reaction results revealed the significantly lower level of *Icam-1* expression in the Exo-srIκB treatment group compared with that in the Exo-Naïve treatment group, in both the pretreatment and post-treatment models (Figure 4c). This result was reproduced in the translational level via Western blotting and immunohistochemical staining (Figure 4d and e). Thus, systemic Exo-srIκB delivery can downregulate the expression of proinflammatory cytokines, chemokines, and adhesion molecules in IR-induced AKI.

Exo-srIκB alleviates apoptosis in post-ischemic kidneys

Based on the well-known role of NF-κB in modulating programmed cell death, we investigated how Exo-srIκB affected apoptosis in post-ischemic kidneys. Kidney IRI surgery induced significant apoptosis in renal cells, which showed an abrupt increase in cleaved caspase-3 and cleaved Poly (adenosine diphosphate–ribose) polymerase (PARP) levels in Western blot analysis. Systemic delivery of Exo-srIκB either before or after the injury could substantially downregulate the expression level of cleaved caspase-3 and cleaved PARP, suggesting that Exo-srIκB has protective effects on apoptosis in post-ischemic kidneys (Figure 5a). Terminal deoxynucleotidyl transferase dUTP nick-end labeling staining was used to determine the extent of renal cell injury. Compared with the controls, Exo-srIκB–treated kidneys showed a significantly lower number of terminal deoxynucleotidyl transferase dUTP nick-end labeling–positive cells in the pretreatment and post-treatment models (Figure 5b).

Biodistribution of exosomes after renal IRI

Next, we investigated the biodistribution of Exo-srIκB in the renal IRI model, to better understand which cell types are orchestrating the protective effect of Exo-srIκB in post-ischemic kidneys. Mice were i.v. injected with fluorochrome-labeled lymphocyte antigen 6 complex, locus G (Ly-6G) and F4/80 antibodies 1 hour before IRI surgery, and i.v. injected with 9×10^9 pn of Exo-srIκB 1 hour after reperfusion. Intravital imaging was performed at 10 minutes, 5 hours, and 24 hours after reperfusion (Figure 6a). Intravital imaging following injection of DiD (green)-labeled exosomes as well as anti–Ly-6G antibody to visualize neutrophils (Fluor 555, red) and anti-F4/80 antibody to visualize macrophages (Fluor 488, blue) confirmed that both Exo-srIκB and Exo-Naïve are taken up by neutrophils ($Ly\text{-}6G^+$) and macrophages ($F4/80^+$) in post-ischemic kidneys (Figure 6b and Supplementary Figure S1A). We observed a mild increase in DiD signal in renal tubules after IRI, raising the possibility of exosome uptake by renal tubular cells, but the signal intensity was not significantly increased compared to the intensity before DiD-labeled exosome injection (data not shown). Spleens were observed at the same time and showed exosomal uptake in the neutrophils and macrophages in the outer parenchymal area (Figure 6c and Supplementary Figure S1B). The inner parenchymal area did not show any significant uptake (data not shown). Due to the limitations of intravital imaging, which allows observation of only superficial regions, we additionally performed immunohistochemical staining to examine the extent of exosome delivery, especially in the outer medulla, which is known to be the site of the most prominent immune cell infiltration in post-ischemic kidneys.[26] We confirmed the successful delivery of $mCherry^+$ Exo-srIκB to the outer medulla of IR-injured kidneys (Supplementary Figure S1C).

Figure 3 | (continued) decreased NF-κB expression, compared with that of the control group (pretreatment 24-hours [h], n = 5–8; pretreatment 48-h, n = 4–5; post-treatment 24-h, n = 5–10; post-treatment 48-h, n = 4–11). Comparisons between groups were assessed using one-way analysis of variance with Bonferroni *post hoc* test. Data are represented as mean ± SD values. $^{***}P < 0.001$ for comparison of the Exo-Naïve-Sham (control) and Exo-Naïve-IRI surgery groups. $^{\#}P < 0.05$, $^{\#\#}P < 0.01$, $^{\#\#\#}P < 0.001$ for comparison of the Exo-Naïve-IRI and Exo-srIκB-IRI surgery groups. HPF, high-power field. To optimize viewing of this image, please see the online version of this article at www.kidney-international.org.

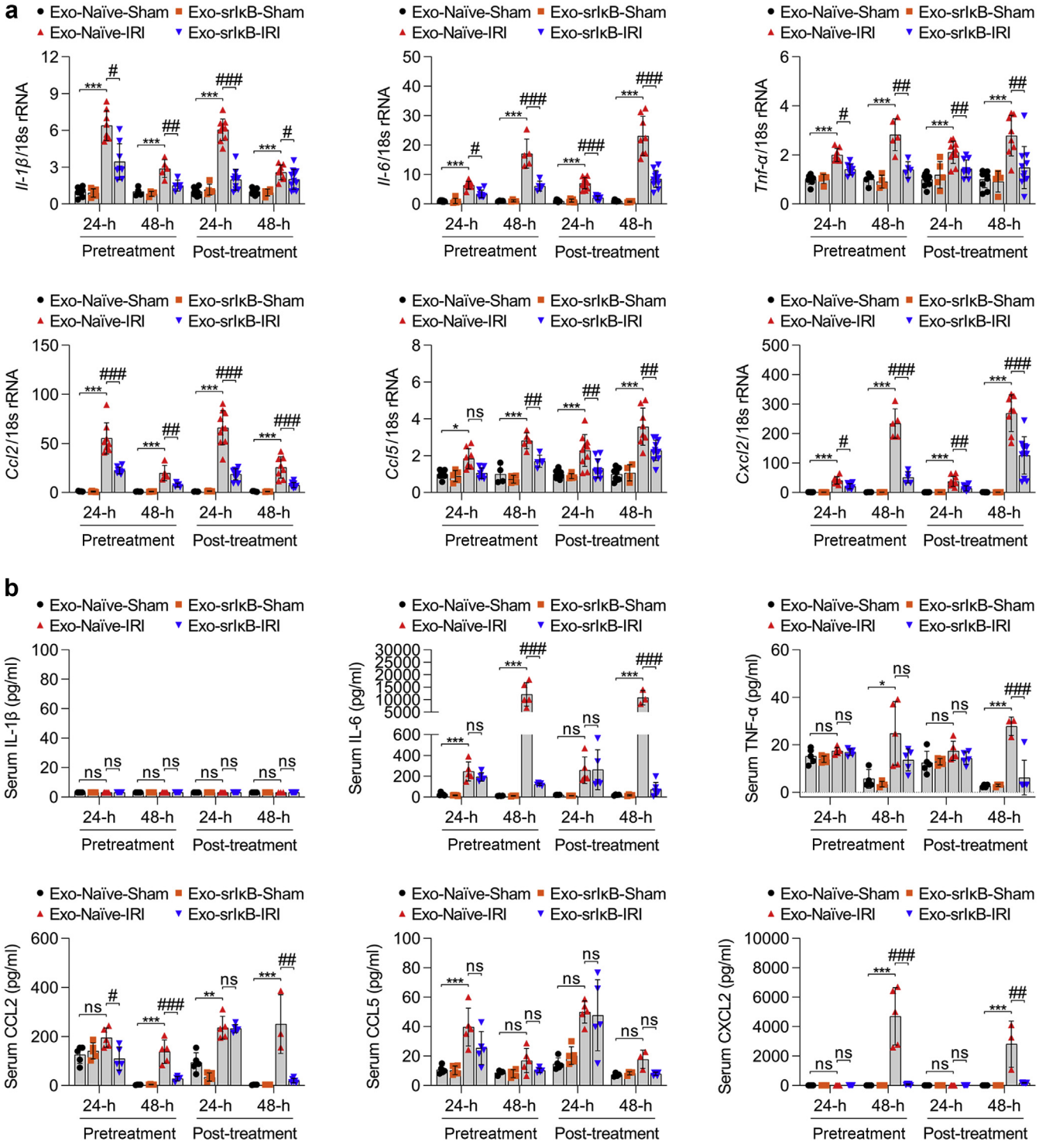

Figure 4 | The expression of proinflammatory cytokines, chemokines, and adhesion molecules is negatively affected by super-repressor kappaB inhibitor–loaded exosome (Exo-srIκB) treatment, both locally and systemically. (**a**) Whole kidney lysates from each experimental group were used for quantitative real-time polymerase chain reaction to measure expression levels of proinflammatory cytokines, including *Il-1β*, *Il-6*, *Tnf-α*, *Ccl2*, *Ccl5*, and *Cxcl2*. The mRNA levels of those genes increased significantly after ischemia–reperfusion (IR) damage in the kidney, and this effect was alleviated with Exo-srIκB treatment (pretreatment 24 hours [h], n = 5–8; pretreatment 48-h, n = 4–5; post-treatment 24-h, n = 5–10; post-treatment 48-h, n = 4–11). (**b**) Multiplex cytokine studies using serum from each experimental group also showed a similar tendency of reduction in proinflammatory cytokine levels in the post-ischemic mouse group with Exo-srIκB treatment (pretreatment 24-h, n = 5; pretreatment 48-h, n = 4–5; post-treatment at 24-h, n = 5; post-treatment 48-h, n = 3–6). (Continued)

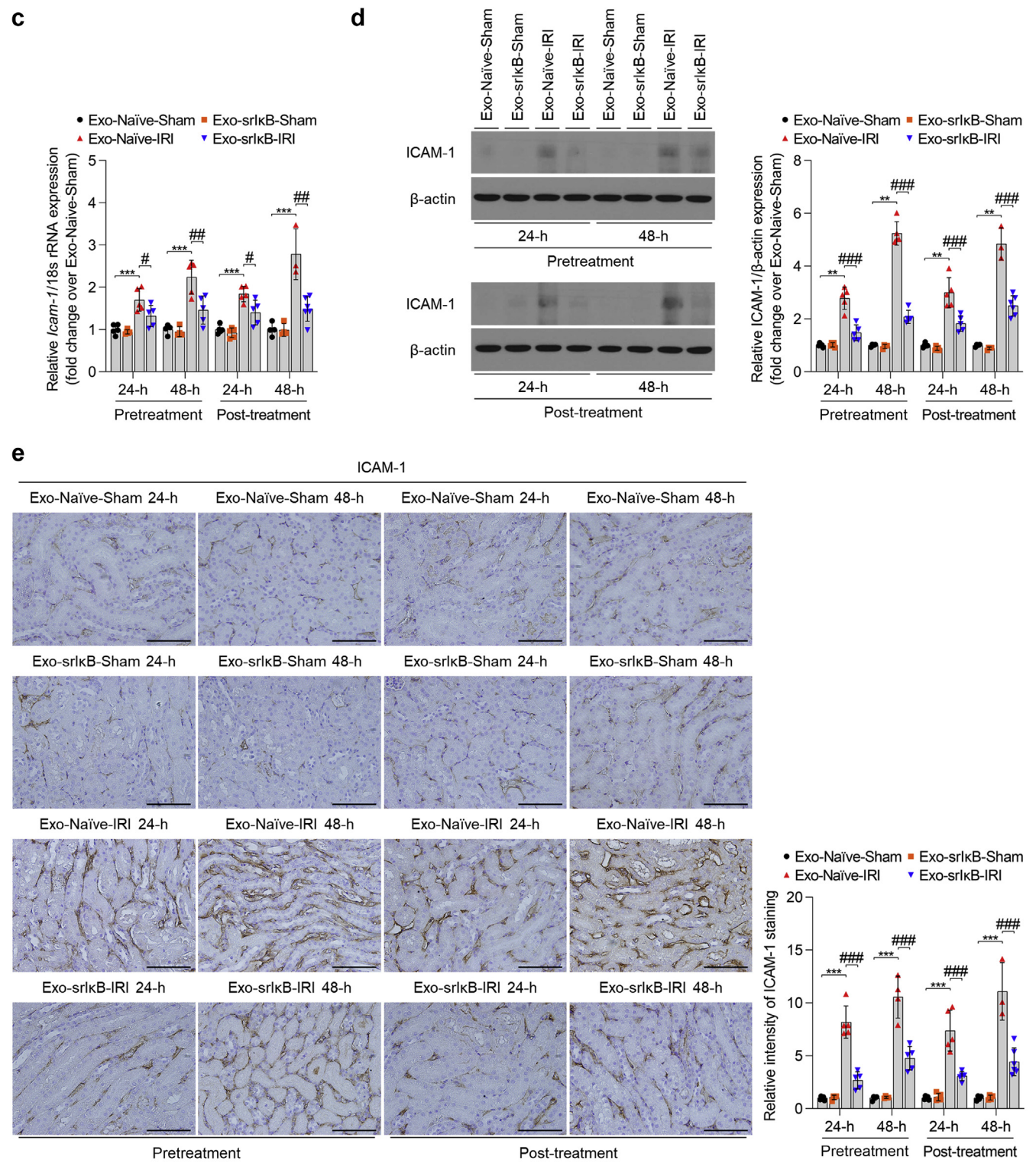

Figure 4 | (Continued) (**c**) Quantitative real-time polymerase chain reaction data show increased levels of *Icam-1* mRNA in the post-ischemic Exo-Naïve (control) treatment group, and significant reduction of *Icam-1* mRNA with Exo-srIκB treatment. (**d**) Western blot analysis results of whole kidney lysates from each group demonstrated decreased expression of ICAM-1 in IR-injured kidneys with Exo-srIκB treatment. (**e**) Representative kidney sections exhibiting ICAM-1 immunohistochemical staining (left) and the graphical representation of ICAM-1 immunohistochemical (right) show that Exo-srIκB treatment reduced ICAM-1 expression in post-ischemic kidneys of C57BL/6J mice. Bar = 50 μm (**c–e**: pretreatment 24-h, n = 5; pretreatment 48-h, n = 4–5; post-treatment 24-h, n = 5; post-treatment 48-h, n = 3–6). Comparisons between groups were assessed using one-way analysis of variance with Bonferroni *post hoc* test. Data are represented as mean ± SD values. $^{*}P < 0.05$, $^{**}P < 0.01$, $^{***}P < 0.001$ for comparisons of the Exo-Naïve-Sham and Exo-Naïve-ischemia–reperfusion (IRI) surgery groups. $^{\#}P < 0.05$, $^{\#\#}P < 0.01$, $^{\#\#\#}P < 0.001$ for comparisons of the Exo-Naïve-IRI and Exo-srIκB-IRI surgery groups. To optimize viewing of this image, please see the online version of this article at www.kidney-international.org.

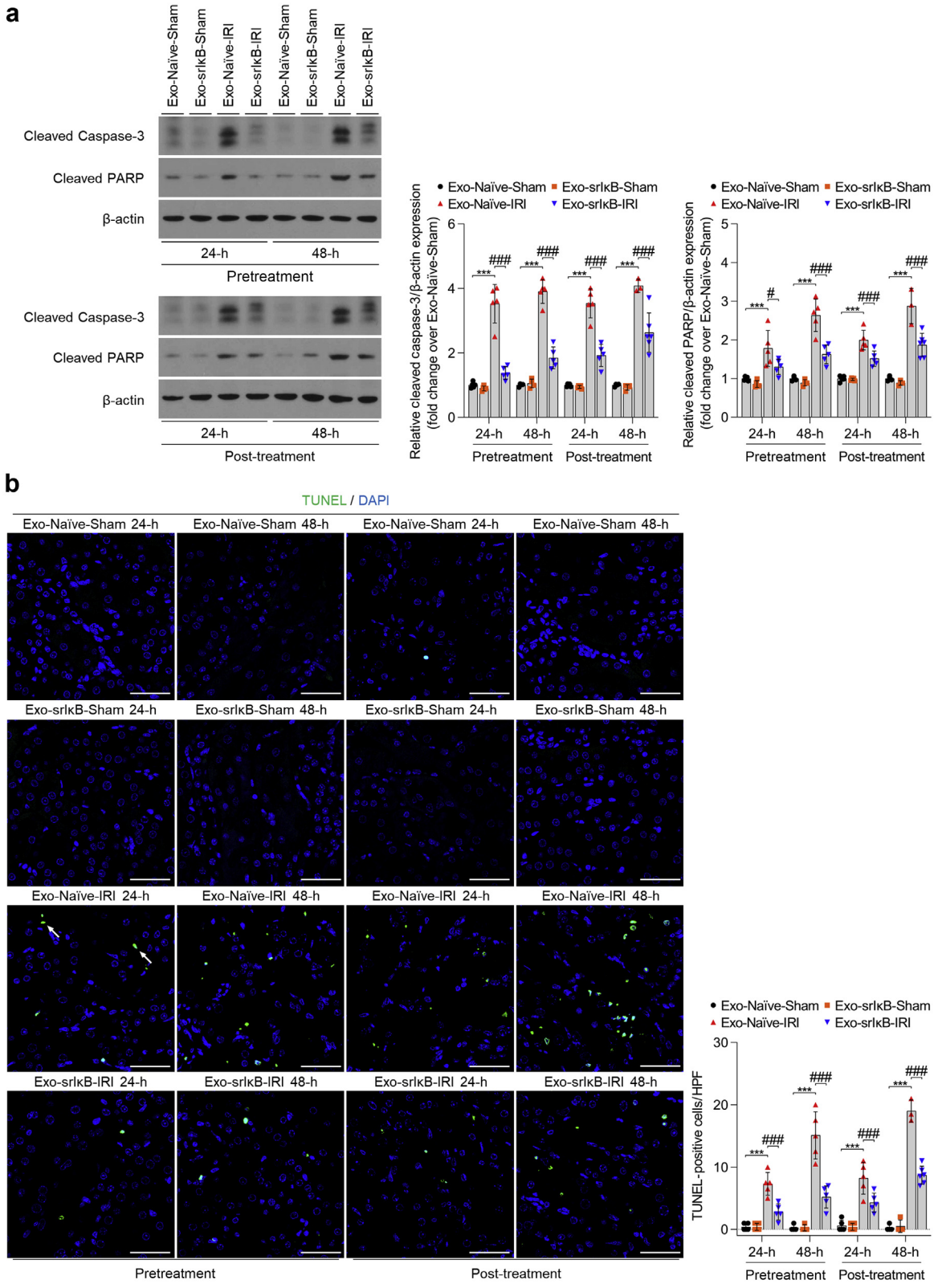

Figure 5 | Super-repressor kappaB inhibitor–loaded exosome (exo-srIκB) treatment improves ischemia–reperfusion (IR)–induced kidney apoptosis. (**a**) (Left) Western blot analysis results comparing the expression of cleaved caspase-3 and cleaved poly (adenosine diphosphate–ribose) polymerase (PARP) protein in kidneys from each experimental group. (Right) Graphical representation shows that Exo-srIκB treatment lowered cleaved caspase-3 levels and cleaved PARP, compared with the Exo-Naïve (control) treatment. (**b**) (Left) Representative images of terminal deoxynucleotidyl transferase dUTP nick-end labeling (TUNEL) staining (fluorescein isothiocyanate–labelled) are shown. Apoptotic cells are green (white arrows), and 4′,6-diamidino-2-phenylindole (DAPI) was used as a counterstain. (Continued)

Systemic delivery of Exo-srIκB affects the renal immune cell population after kidney IRI

Based on the biodistribution data, we evaluated whether providing exosomal srIκB treatment before IRI surgery could affect the population of each immune cell type. After 24 hours of ischemic AKI, there was no difference between the experimental groups in the total number of renal cells isolated through multiple steps of mechanical disruption, enzymatic digestion, and the Percoll density gradient method, but the Exo-srIκB–treated group had a significantly lower frequency of kidney mononuclear cells than did the Exo-Naïve–treated group ($P < 0.05$; Figure 7a and b). Further analysis showed that the Exo-srIκB–injected group had a significantly lower frequency of neutrophils ($CD45^+Ly\text{-}6G^+$; $P < 0.01$), pro-inflammatory mononuclear phagocytic cells ($CD45^+Ly\text{-}6C^+$), anti-inflammatory mononuclear phagocytic cells ($CD45^+F4/80^+$; $P < 0.01$ and $P < 0.05$, respectively), and T cells ($CD45^+CD3^+$; $P < 0.05$) among total kidney mononuclear cells than those in the Exo-Naïve–injected group (Figure 7c). Results of immunofluorescence of IR-damaged kidneys also showed decreased neutrophil and mononuclear phagocytic cell frequencies in Exo-srIκB–injected kidneys (Figure 7d–f and Supplementary Figure S2A–C). However, Exo-srIκB treatment did not have significant effects on the total immune cell numbers or frequencies in the spleen after ischemic AKI. There were no differences in numbers and frequencies of total immune cells ($CD45^+$), neutrophils ($CD45^+Ly\text{-}6G^+$), pro- or anti-inflammatory mononuclear phagocytic cells ($CD45^+Ly\text{-}6C^+$ or $CD45^+F4/80^+$), except T cells ($CD45^+CD3^+$) between the Exo-srIκB and Exo-Naïve treatment groups (Supplementary Figure S3A–C). This suggests that systemic Exo-srIκB treatment before ischemic AKI has significant local effects on renal immune cell proliferation and trafficking, but not on splenic immune cells.

DISCUSSION

Despite recent noteworthy advancements in understanding of the pathophysiology of IR-induced AKI, no drug with proven clinical efficacy and safety to treat ischemic AKI has been developed; thus, the associated mortality and morbidity levels are significant. Given that NF-κB signaling is deeply involved in the course of IR-induced AKI,[27] we assessed whether the systemic delivery of the NF-κB inhibitor using exosomes could alleviate the course of ischemic AKI. Through optogenetically controlled biogenesis of exosomes using EXPLOR technology, we delivered Exo-srIκB to mice either before or after IRI surgery and compared outcomes with those of the control group. Our results show that the mouse group receiving the Exo-srIκB treatment was protected from IR-induced AKI; this group showed better biochemical and histologic outcomes than the control group. Systemic delivery of Exo-srIκB suppressed NF-κB signaling in post-ischemic kidneys, which led to decreased expression of proinflammatory cytokines, chemokines, and adhesion molecules and alleviation of apoptosis. Finally, we compared whether NF-κB treatment affected the renal immune cell population and observed a significant reduction in frequencies of multiple immune cell populations, including neutrophils, monocytes, macrophages, and T cells, through flow cytometric and immunofluorescent analysis.

During the early course of IRI, proinflammatory cascade and oxidative stress results in NF-κB pathway activation, subsequently leading to the regulation of cell survival and inflammation.[28] Multiple endogenous factors are released during the early stages of hypoxia and reperfusion, including high mobility group box 1, heat shock proteins, pathogen-associated molecular patterns, and damage-associated molecular patterns,[29] and these molecules stimulate pattern recognition receptors, such as Toll-like receptors and the interleukin-1 receptor. This process subsequently activates IκB kinase, which leads to IκB degradation by proteasomes.[27] Next, heterodimers (e.g., p50/p65) translocate from the cytosol to the nucleus, where they promote the transcription of inflammatory mediators, including tumor necrosis factor–α, IL-1, IL-6, and IL-8, which in turn further promote NF-κB signaling.[27,30,31] This proinflammatory cascade modulates surrounding microenvironments, by inducing apoptosis in renal tubular cells subjected to IRI and promoting leukocyte migration and activation. Our experimental ischemic AKI model could reproduce the activation of NF-κB signaling following renal IRI, leading to the increased expression of multiple inflammatory cytokines, chemokines, and tissue apoptosis, which significantly affect renal immune cell populations.

Recent experimental studies have shown more detailed evidence regarding the effect of NF-κB blockade on IRI, using selective pharmacologic inhibitors of NF-κB signaling, including Toll-like receptor antagonists,[32,33] cytokine antagonists,[34] IKK complex antagonists,[35,36] proteasome inhibitors,[37] and decoy oligodeoxynucleotides specific to a particular NF-κB complex,[15,38,39] in various organs. srIκB is a nondegradable IκBα protein with mutations at serine residues 32 and 36. This protein prevents NF-κB nuclear translocation and subsequent NF-κB signaling.[40] srIκB has proven protective effects in the lung IRI model, as it decreases neutrophil infiltration and pulmonary edema, and is also known to have anti-tumor effects, because it decreases chemoresistance.[41,42] Recently, Markó *et al.* generated mice expressing srIκB in

Figure 5 | (Continued) Bar = 50 μm. (Right) A bar graph showing TUNEL-positive cells in kidney sections from each group. Exo-srIκB treatment induced a lower number of apoptotic cells (pretreatment 24-hours [h], n = 5; pretreatment 48-h, n = 4–5; post-treatment 24-h, n = 5; post-treatment 48-h, n = 3–6). Comparisons between groups were assessed using one-way analysis of variance with the Bonferroni *post hoc* test. Data are represented as mean ± SD values. $^{***}P < 0.001$ for comparison of the Exo-Naïve-Sham and Exo-Naïve-IR injury (IRI) surgery groups. $^{\#}P < 0.05$ and $^{\#\#\#}P < 0.001$ for comparison of the Exo-Naïve-IRI and Exo-srIκB-IRI surgery groups. To optimize viewing of this image, please see the online version of this article at www.kidney-international.org.

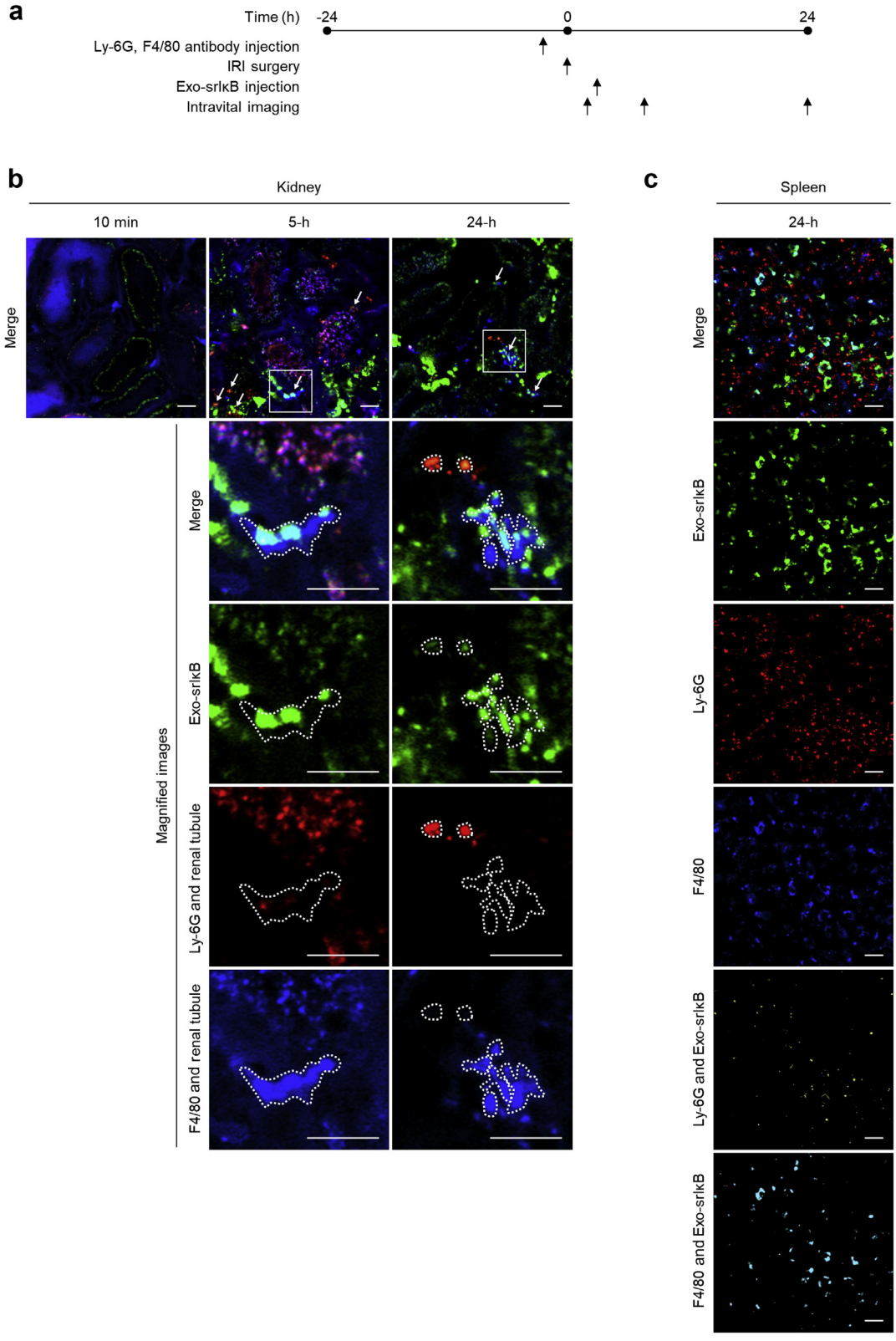

Figure 6 | Super-repressor kappaB inhibitor–loaded exosome (Exo-srIκB) primarily target immune cells in post-ischemic kidneys. (**a**) Experimental scheme of intravital imaging and exosome delivery. (**b**) Sequential intravital imaging shows the uptake of 1,1′-dioctadecyl-3,3,3′,3′-tetramethylindodicarbocyanine, 4-chlorobenzenesulfonate salt (DiD)–labeled exosome (green pseudocolor) into neutrophils (Ly-6G$^+$, red pseudocolor) and macrophages (F4/80$^+$, blue pseudocolor) in the post-ischemic kidneys treated with i.v. Exo-srIκB. White arrows indicate DiD-labeled exosomes engulfed in immune cells. White dashed lines indicate renal interstitium. (**c**) The biodistribution of DiD-labeled exosomes (green) in the spleen after kidney ischemia–reperfusion injury surgery shows exosomal uptake into neutrophils (Ly-6G$^+$, red) and macrophages (F4/80$^+$, blue) in the outer parenchyma. Elapsed time is indicated. Bar = 20 μm. To optimize viewing of this image, please see the online version of this article at www.kidney-international.org.

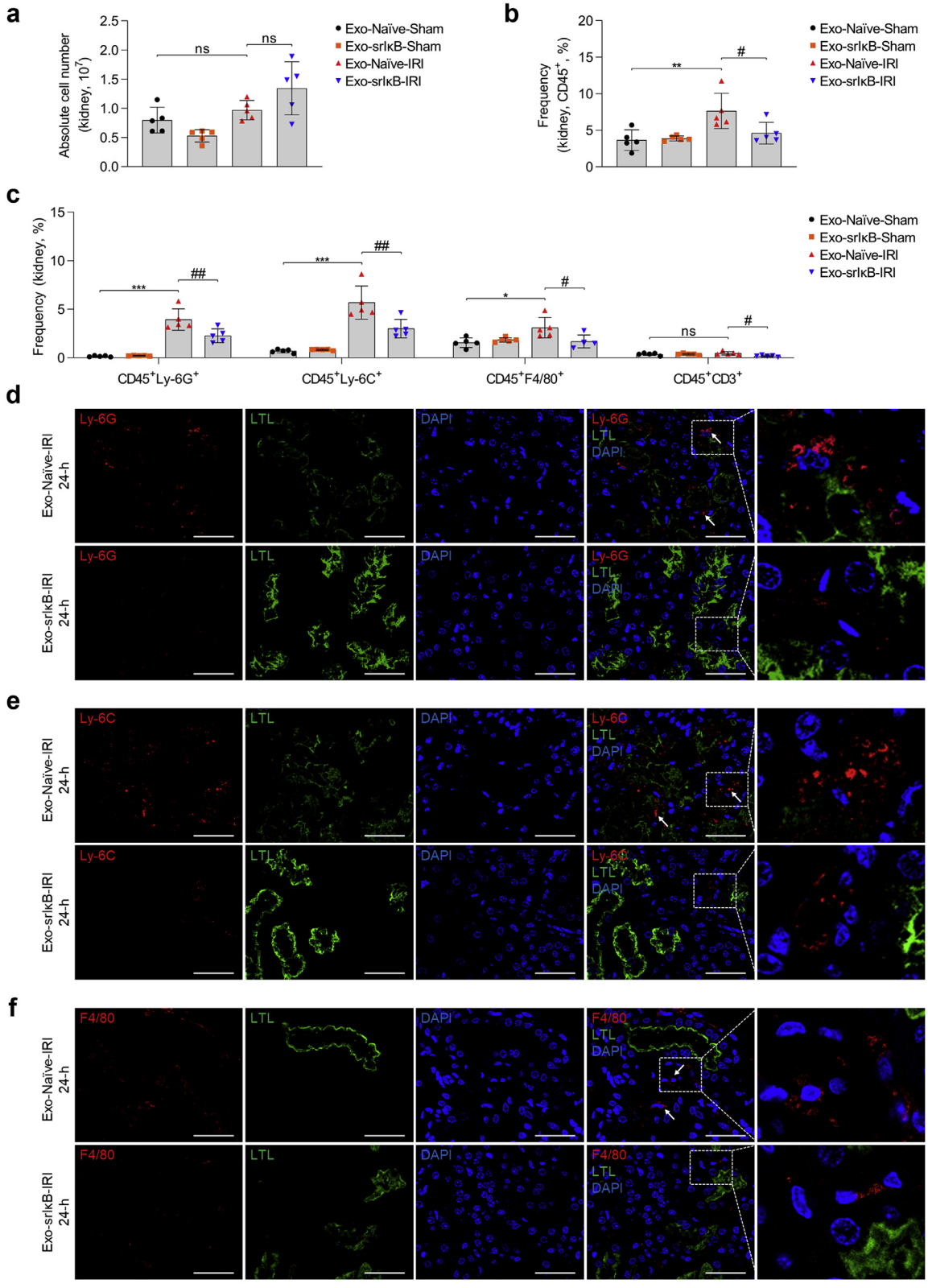

Figure 7 | Super-repressor kappaB inhibitor–loaded exosome (Exo-srIκB) treatment modulates kidney immune cell populations following ischemia–reperfusion (IR)–induced acute kidney injury. (**a**) Mice were sacrificed 24 hours (h) after surgery. Kidney mononuclear cells were enriched using enzymatic digestion, mechanical disruption, and Percoll density gradients. Total kidney cell numbers determined using those methods showed no statistical differences among the experimental groups. (**b**) Graphical representation of flow cytometric analysis showed a higher percentage of kidney $CD45^+$ cells after IR injury among isolated kidney cells using enzymatic digestion, mechanical disruption, and Percoll density gradients. Exo-srIκB treatment alleviated the post-ischemic surge of renal immune cells. (Continued)

renal tubular cells, and these mice were protected from ischemic AKI.[43] By using bioengineered exosomes as a vector, Choi *et al.* recently showed the therapeutic benefits of srIκB treatment in the septic AKI model.[25] Our study also demonstrates the protective effects of Exo-srIκB treatment in the renal IRI model, expanding the therapeutic potential of srIκB delivery through exosomes in various types of AKI.

Modulation of the inflammatory process has been a major therapeutic consideration in the field of ischemic AKI. A study by Nagata *et al.* showed that splenectomy, as well as use of the anti-TNF-α agent infliximab, showed protective effects in the experimental ischemic AKI model, by lowering inflammatory cytokine expression and accumulation of monocytes and macrophages.[44] Inoue *et al.*, on the other hand, showed that vagus nerve stimulation could protect kidneys from ischemic AKI through the cholinergic anti-inflammatory pathway.[45] However, splenectomy had no effect on the course of ischemic AKI in this study. Inhibiting the migration of leukocytes and macrophages also preserved renal function and alleviated cell death.[46,47] We have shown that Exo-srIκB treatment downregulates the expression of proinflammatory cytokines, chemokines, and adhesion molecules, reduces apoptosis, and alleviates multi-lineage immune cell accumulation in IR-injured kidneys. These results suggest that Exo-srIκB modifies the course of ischemic AKI through proinflammatory cascade downregulation, limiting subsequent migration and activation of leukocytes, and preventing apoptosis.

Exosomes can have several advantages over the use of other types of vectors as conveyors. First, extracellular vesicles are naturally protected from degradation during circulation and are non-immunogenic when used autologously.[48] Exosomes can overcome natural barriers, such as the blood–brain barrier, through their intrinsic cell-targeting properties.[49] Additionally, exosomes use intrinsic mechanisms of recipient cells in the course of uptake, intracellular trafficking, and the final delivery of cargoes to target cells.[50] While maintaining these properties, EXPLOR technology made it possible to significantly increase intracellular levels of cargo proteins through controllable, reversible detachment from exosomes.[24] Our study showed that efficient delivery of Exo-srIκB using EXPLOR technology could bring significant improvement in renal outcome after experimental IRI. Also, our preliminary toxicity data with 1.0×10^{10} pn of Exo-srIκB did not show any significant adverse reaction (data not shown).

Our study showed that exosomal srIκB treatment could suppress NF-κB signaling in post-ischemic kidneys and lead to a decreased level of inflammation and apoptosis. It is so far uncertain whether these effects originate primarily from NF-κB signaling modulation in renal tubular cells or secondarily from regulating NF-κB signaling in immune cells. However, our bio-distribution data showed more vigorous exosomal uptake in neutrophils and macrophages, and our previous study also showed prompt exosomal uptake in immune cells—within a few minutes, which differs from other major organs, including kidney, which takes several hours to reach its peak uptake of exosomes.[25] Therefore, it seems reasonable to postulate that these protective effects from Exo-srIκB treatment in ischemic AKI are primarily mediated by the immune cells. Further *in vivo* studies using immunodeficient mice or *in vitro* co-culture studies of tubular cells with or without immune cells under ischemic conditions will be able to provide additional answers to this question.

Of note, exosomes were delivered through the i.p. route in most of our studies. However, the pilot study for intravital imaging showed significant aggregation of exosomes after i.p. injection, limiting accurate interpretation. Therefore, the i.v. route was chosen for the bio-distribution study. To determine whether similar protective effects from i.p. exosomal delivery are found with i.p. delivery, we repeated some experiments using the i.v. injection method. We were able to reproduce the improved biochemical outcomes, as well as the decreased level of NF-κB signaling and intercellular adhesion molecule 1-1 expression, with i.v. delivery of Exo-srIκB (Supplementary Figure S4).

Our study has several limitations. First, our study is limited to the murine model. Future *in vivo* renal IRI experiments using humanized mice, or *in vitro* hypoxia–reperfusion experiments using human monocytes will need to be conducted to assess the therapeutic potential of human applications. Also, our experiment focused on only the early stages of renal IRI. However, several recent studies have highlighted the significant role of NF-κB signaling in hypoxia-induced renal fibrosis, via the effects on the regulation of inflammation, oxidative stress, and epithelial-to-mesenchymal transition.[43,51] Additional experiments focusing on the effects of Exo-srIκB in renal fibrosis and the repair process after IRI would potentially broaden the clinical applicability of Exo-srIκB treatment.

In conclusion, our study shows that using the exosome as a carrier is a safe and efficient method for delivering srIκB into the IR-induced AKI model. Exo-srIκB treatment alleviates IR-induced AKI in mice by downregulating NF-κB signaling and ameliorating inflammation and apoptosis in the ischemic

Figure 7 | (Continued) (**c**) Results of further staining with additional immune-cell markers showed that the frequency of multilineage immune cells, including neutrophils ($CD45^+Ly\text{-}6G^+$), pro-inflammatory mononuclear phagocytic cells ($CD45^+Ly\text{-}6C^+$), anti-inflammatory mononuclear phagocytic cells ($CD45^+F4/80^+$), and T cells ($CD45^+CD3^+$), among enriched kidney mononuclear cells were also decreased with Exo-srIκB treatment in post-ischemic kidneys (n = 5 per each experimental group). (**d**–**f**) Immunofluorescence studies were performed on post-ischemic kidneys from each experimental group, targeting Ly-6G, Ly-6C, and F4/80. Secondary antibodies conjugated with Alexa Fluor 647 were used for all immunofluorescence experiments. Data showed a decreased frequency of Alexa Fluor 647 stained cells (white arrows) in post-ischemic kidneys following Exo-srIκB treatment, suggesting that there were fewer neutrophils ($Ly\text{-}6G^+$), pro-, and anti-inflammatory mononuclear phagocytic cells ($Ly\text{-}6C^+F4/80^+$) in Exo-srIκB-treated kidneys. Proximal tubular cells were stained with lotus tetragonolobus lectin (green), and 4′,6-diamidino-2-phenylindole was used for counterstaining. Bar = 50 μm (n = 5 per experimental group). Data are represented as mean ± SD values. $^*P < 0.05$, $^{**}P < 0.01$, $^{***}P < 0.001$ for comparisons of the Exo-Naive-Sham and Exo-Naive-ischemia–reperfusion (IRI) surgery groups. $^{\#}P < 0.05$, $^{\#\#}P < 0.01$ for comparisons of the Exo-Naive-IRI and Exo-srIκB-IRI surgery groups. To optimize viewing of this image, please see the online version of this article at www.kidney-international.org.

injured kidney. The direct intracellular delivery of immunosuppressive proteins into target cells using exosomes can be used as a promising therapeutic tool in IR-induced AKI, and the therapeutic potential of Exo-srIκB in human kidney IRI should be explored further.

DISCLOSURE

T-HY and JIY are Scientific Advisory Board members at ILIAS Biologics Inc. Both Korean Republic and US patent applications related to this work were filed in 2020. CC is the founder and shareholder of ILIAS Biologics Inc, and S-H A, CHP, and J-KY are minor shareholders of ILIAS Biologics Inc. All the other authors declared no competing interests.

ACKNOWLEDGMENTS

This work was supported by grants from the National Research Foundation of Korea (NRF-2017R1A2B4005720, NRF-2017R1A2B3002241, NRF-2018M3A9E2022820, NRF-2019R1A2C2084535, NRF-2020R1I1A1A01072977), which is funded by the Korean government (MSIP and MOE). This study was also supported by ILIAS Biologics Inc., based on the Sponsored Research Agreement (SRA) between MET Inc. and ILIAS Biologics Inc., and Yonsei University College of Medicine and ILIAS Biologics Inc. The authors thank Medical Illustration & Design, part of the Medical Research Support Services of Yonsei University College of Medicine, for all artistic support related to this work.

AUTHOR CONTRIBUTIONS

SK and T-HY conceived and designed the project, and JIY, CC, and T-HY supervised and developed the study. SK, SAL, HY, MYK, J-KY, S-HA, NHK, and HSK conducted experiments. SK and SAL acquired data. SK, JP, BYN, and JIY analyzed data, and SK and SAL wrote the manuscript. T-HY, CHP, J-KY, JTP, SHH, and S-WK reviewed the manuscript and provided suggestions for further development.

SUPPLEMENTARY MATERIAL

Supplementary File (PDF)

Supplementary Methods.

Table S1. Primer sequences.

Figure S1. Intravital imaging of Exo-Naïve and successful delivery of Exo-Naïve into outer medulla in post-ischemic kidneys. (**A**) Sequential intravital imaging shows the uptake of DiD-labeled exosome (green pseudocolor) into neutrophils (Ly-6G+, red pseudocolor) and macrophages (F4/80+, blue pseudocolor) in the post-ischemic kidneys treated with i.v. Exo-Naïve. White dashed line indicates renal interstitium. (**B**) The biodistribution of DiD-labeled exosomes (green) in spleen after kidney IRI surgery shows exosomal uptake into neutrophils (Ly-6G+, red) and macrophages (F4/80+, blue) in the outer parenchyma. Elapsed time is indicated. Bar = 20 μm. (**C**) Representative kidney sections of mCherry immunohistochemical staining showing Exo-srIκB in the outer medulla of post-ischemic kidneys. Red dashed line indicates the existence of mCherry^{+} srIκB. The control group did not receive any exosome treatment. Bar = 20 μm.

Figure S2. Exo-srIκB treatment has no effect on kidney immune cell populations following sham surgery. (**A–C**) Immunofluorescence studies were performed after sham surgery from each experimental group, targeting Ly-6G, Ly-6C, and F4/80. Secondary antibodies conjugated with Alexa Fluor 647 were used for all immunofluorescence experiments. Data showed no significant immune cell infiltration in both Exo-Naïve-Sham and Exo-srIκB-Sham groups. Ly-6G^{+}, Ly-6C^{+}and F4/80^{+} were stained with Alexa Fluor 647 (red), proximal tubular cells were stained with LTL (green), and DAPI was used for counterstaining. Bar = 50 μm.

Figure S3. Exo-srIκB treatment has no effect on splenic immune cell populations following ischemic AKI. (**A,B**) Splenocytes were isolated via mechanical digestion. Results of flow cytometric analysis showed no significant differences in (**A**) total splenocyte counts and (**B**) frequencies of CD45^{+} cells among the total splenocytes between experimental groups. (**C**) The frequencies of splenic neutrophils (CD45^{+}Ly-6G^{+}) and pro-inflammatory (CD45^{+}Ly-6C^{+}) as well as anti-inflammatory mononuclear phagocytic cells (CD45^{+}F4/80^{+}) increased after kidney IRI, but treatment with Exo-srIκB did not cause differences between the Exo-Naïve and Exo-srIκB treatment groups. Frequencies of splenic T cells (CD45^{+}CD3^{+}) remained unchanged after kidney IRI, and Exo-srIκB treatment slightly increased splenic T cell frequencies, compared with those in the Exo-Naïve treatment group (n = 5 per experimental group). Comparisons between groups were assessed using one-way ANOVA with the Bonferroni *post hoc* test. Data are represented as mean ± SD values. $^{*}P < 0.05$, $^{**}P < 0.01$, $^{***}P < 0.001$, for comparisons of the Exo-Naïve-Sham and Exo-Naïve-IRI surgery groups. $^{\#}P < 0.05$, for comparison of the Exo-Naïve-IRI and Exo-srIκB-IRI surgery groups.

Figure S4. I.v. delivery of Exo-srIκB shows similar biologic effects compared to i.p. delivery in the ischemic AKI model. (**A**) Experimental scheme of kidney IRI surgery and exosome delivery. Each mouse group was i.v. injected with 9×10^{9} pn of Exo-Naïve, Exo-srIκB, or PBS 1 hour after reperfusion. Mice were killed either 24 or 48 hours after IRI surgery, and serum and tissues were collected for further evaluation. (**B–D**) Serum levels of BUN, creatinine, and NGAL among different groups depending on treatment type (PBS vs. Exo-Naïve vs. Exo-srIκB), renal injury (sham vs. IRI), and follow-up time point (24-h and 48-h), which shows the renal protective effect of Exo-srIκB treatment (n = 5 per experimental group). (**E**) Western blot analysis of NF-κB p65 expression using renal nuclear extracts from each experimental mouse group. Nuclear extracts were biochemically separated from cytoplasmic fractions, and NF-κB p65 and Lamin B1 expression was analyzed via Western blotting. IRI-induced activation of NF-κB signaling was significantly repressed with postoperative Exo-srIκB treatment. (**F**) Elevated DNA-binding activity of NF-κB p65 following renal IRI was suppressed with postoperative Exo-srIκB treatment. (**G**) qRT-PCR data show increased levels of *Icam-1* mRNA in the post-ischemic Exo-Naïve treatment group and significant reduction of *Icam-1* mRNA with Exo-srIκB treatment. (**H**) Western blot analysis results of whole kidney lysates from each group demonstrated decreased expression of ICAM-1 in IR-injured kidneys with Exo-srIκB treatment. Comparisons between groups were assessed using one-way ANOVA with Bonferroni *post hoc* test. Data are represented as mean ± SD values. ns, not significant, $^{**}P < 0.01$, $^{***}P < 0.001$, for comparison of the PBS-Sham and Exo-Naïve-IRI surgery groups. $^{\#}P < 0.05$, $^{\#\#}P < 0.01$, $^{\#\#\#}P < 0.001$ for comparison of the Exo-Naïve-IRI and Exo-srIκB-IRI surgery groups.

REFERENCES

1. Bonventre JV, Weinberg JM. Recent advances in the pathophysiology of ischemic acute renal failure. *J Am Soc Nephrol*. 2003;14:2199–2210.
2. Lee SA, Cozzi M, Bush EL, et al. Distant organ dysfunction in acute kidney injury: a review. *Am J Kidney Dis*. 2018;72:846–856.
3. Han SJ, Lee HT. Mechanisms and therapeutic targets of ischemic acute kidney injury. *Kidney Res Clin Pract*. 2019;38:427–440.
4. Burne MJ, Daniels F, El Ghandour A, et al. Identification of the CD4(+) T cell as a major pathogenic factor in ischemic acute renal failure. *J Clin Invest*. 2001;108:1283–1290.
5. Tadagavadi RK, Reeves WB. Renal dendritic cells ameliorate nephrotoxic acute kidney injury. *J Am Soc Nephrol*. 2010;21:53–63.
6. Akcay A, Nguyen Q, He Z, et al. IL-33 exacerbates acute kidney injury. *J Am Soc Nephrol*. 2011;22:2057–2067.
7. Lee SA, Noel S, Sadasivam M, et al. Role of immune cells in acute kidney injury and repair. *Nephron*. 2017;137:282–286.

8. Smith SF, Hosgood SA, Nicholson ML. Ischemia-reperfusion injury in renal transplantation: 3 key signaling pathways in tubular epithelial cells. *Kidney Int*. 2019;95:50–56.
9. Gupta SC, Sundaram C, Reuter S, et al. Inhibiting NF-κB activation by small molecules as a therapeutic strategy. *Biochim Biophys Acta*. 2010;1799:775–787.
10. Ruiz-Ortega M, Bustos C, Hernández-Presa MA, et al. Angiotensin II participates in mononuclear cell recruitment in experimental immune complex nephritis through nuclear factor-kappa B activation and monocyte chemoattractant protein-1 synthesis. *J Immunol*. 1998;161:430–439.
11. Sanz AB, Justo P, Sanchez-Niño MD, et al. The cytokine TWEAK modulates renal tubulointerstitial inflammation. *J Am Soc Nephrol*. 2008;19:695–703.
12. Sanz AB, Sanchez-Niño MD, Ramos AM, et al. NF-kappaB in renal inflammation. *J Am Soc Nephrol*. 2010;21:1254–1262.
13. Kim KH, Lee ES, Cha SH, et al. Transcriptional regulation of NF-kappaB by ring type decoy oligodeoxynucleotide in an animal model of nephropathy. *Exp Mol Pathol*. 2009;86:114–120.
14. Vos IH, Govers R, Grone HJ, et al. NFkappaB decoy oligodeoxynucleotides reduce monocyte infiltration in renal allografts. *FASEB J*. 2000;14:815–822.
15. Cao CC, Ding XQ, Ou ZL, et al. In vivo transfection of NF-kappaB decoy oligodeoxynucleotides attenuate renal ischemia/reperfusion injury in rats. *Kidney Int*. 2004;65:834–845.
16. Li X, Ding L, Xu Y, et al. Targeted delivery of doxorubicin using stealth liposomes modified with transferrin. *Int J Pharm*. 2009;373:116–123.
17. Moritake S, Taira S, Ichiyanagi Y, et al. Functionalized nano-magnetic particles for an in vivo delivery system. *J Nanosci Nanotechnol*. 2007;7:937–944.
18. Puar YR, Shanmugam MK, Fan L, et al. Evidence for the involvement of the master transcription factor NF-κB in cancer initiation and progression. *Biomedicines*. 2018;6:82.
19. Wold WS, Toth K. Adenovirus vectors for gene therapy, vaccination and cancer gene therapy. *Curr Gene Ther*. 2013;13:421–433.
20. Szebeni J, Moghimi SM. Liposome triggering of innate immune responses: a perspective on benefits and adverse reactions. *J Liposome Res*. 2009;19:85–90.
21. Li SP, Lin ZX, Jiang XY, et al. Exosomal cargo-loading and synthetic exosome-mimics as potential therapeutic tools. *Acta Pharmacol Sin*. 2018;39:542–551.
22. Boukouris S, Mathivanan S. Exosomes in bodily fluids are a highly stable resource of disease biomarkers. *Proteomics Clin Appl*. 2015;9:358–367.
23. Jiang XC, Gao JQ. Exosomes as novel bio-carriers for gene and drug delivery. *Int J Pharm*. 2017;521:167–175.
24. Yim N, Ryu SW, Choi K, et al. Exosome engineering for efficient intracellular delivery of soluble proteins using optically reversible protein-protein interaction module. *Nat Commun*. 2016;7:12277.
25. Choi H, Kim Y, Mirzaaghasi A, et al. Exosome-based delivery of super-repressor IκBα relieves sepsis-associated organ damage and mortality. *Sci Adv*. 2020;6:eaaz6980.
26. Li L, Huang L, Vergis AL, et al. IL-17 produced by neutrophils regulates IFN-gamma-mediated neutrophil migration in mouse kidney ischemia-reperfusion injury. *J Clin Invest*. 2010;120:331–342.
27. Andrade-Oliveira V, Foresto-Neto O, Watanabe IKM, et al. Inflammation in renal diseases: new and old players. *Front Pharmacol*. 2019;10:1192.
28. Wu MY, Yiang GT, Liao WT, et al. Current mechanistic concepts in ischemia and reperfusion injury. *Cell Physiol Biochem*. 2018;46:1650–1667.
29. Valen G, Yan ZQ, Hansson GK. Nuclear factor kappa-B and the heart. *J Am Coll Cardiol*. 2001;38:307–314.
30. Mulero MC, Huxford T, Ghosh G. NF-kappaB, IkappaB, and IKK: integral components of immune system signaling. *Adv Exp Med Biol*. 2019;1172:207–226.
31. Gu L, Tao Y, Chen C, et al. Initiation of the inflammatory response after renal ischemia/reperfusion injury during renal transplantation. *Int Urol Nephrol*. 2018;50:2027–2035.
32. Liu M, Gu M, Xu D, et al. Protective effects of Toll-like receptor 4 inhibitor eritoran on renal ischemia-reperfusion injury. *Transplant Proc*. 2010;42:1539–1544.
33. Farrar CA, Keogh B, McCormack W, et al. Inhibition of TLR2 promotes graft function in a murine model of renal transplant ischemia-reperfusion injury. *FASEB J*. 2012;26:799–807.
34. Gu Q, Yang XP, Bonde P, et al. Inhibition of TNF-alpha reduces myocardial injury and proinflammatory pathways following ischemia-reperfusion in the dog. *J Cardiovasc Pharmacol*. 2006;48:320–328.
35. Onai Y, Suzuki J, Kakuta T, et al. Inhibition of IkappaB phosphorylation in cardiomyocytes attenuates myocardial ischemia/reperfusion injury. *Cardiovasc Res*. 2004;63:51–59.
36. Moss NC, Stansfield WE, Willis MS, et al. IKKbeta inhibition attenuates myocardial injury and dysfunction following acute ischemia-reperfusion injury. *Am J Physiol Heart Circ Physiol*. 2007;293:H2248–H2253.
37. Itoh M, Takaoka M, Shibata A, et al. Preventive effect of lactacystin, a selective proteasome inhibitor, on ischemic acute renal failure in rats. *J Pharmacol Exp Ther*. 2001;298:501–507.
38. Qian JM, Zhang H, Wu XF, et al. Improvement of recipient survival after small size graft liver transplantation in rats with preischemic manipulation or administering antisense against nuclear factor-kappaB. *Transpl Int*. 2007;20:784–789.
39. Latanich CA, Toledo-Pereyra LH. Searching for NF-kappaB-based treatments of ischemia reperfusion injury. *J Invest Surg*. 2009;22:301–315.
40. Yamamoto Y, Gaynor RB. Therapeutic potential of inhibition of the NF-kappaB pathway in the treatment of inflammation and cancer. *J Clin Invest*. 2001;107:135–142.
41. Ishiyama T, Dharmarajan S, Hayama M, et al. Inhibition of nuclear factor kappaB by IkappaB superrepressor gene transfer ameliorates ischemia-reperfusion injury after experimental lung transplantation. *J Thorac Cardiovasc Surg*. 2005;130:194–201.
42. Wang CY, Cusack JC Jr, Liu R, et al. Control of inducible chemoresistance: enhanced anti-tumor therapy through increased apoptosis by inhibition of NF-kappaB. *Nat Med*. 1999;5:412–417.
43. Markó L, Vigolo E, Hinze C, et al. Tubular epithelial NF-κB activity regulates ischemic AKI. *J Am Soc Nephrol*. 2016;27:2658–2669.
44. Nagata Y, Fujimoto M, Nakamura K, et al. Anti-TNF-alpha agent infliximab and splenectomy are protective against renal ischemia-reperfusion injury. *Transplantation*. 2016;100:1675–1682.
45. Inoue T, Abe C, Sung SS, et al. Vagus nerve stimulation mediates protection from kidney ischemia-reperfusion injury through α7nAChR+ splenocytes. *J Clin Invest*. 2016;126:1939–1952.
46. Zuk A, Gershenovich M, Ivanova Y, et al. CXCR(4)antagonism as a therapeutic approach to prevent acute kidney injury. *Am J Physiol Renal Physiol*. 2014;307:F783–F797.
47. Stoppe C, Averdunk L, Goetzenich A, et al. The protective role of macrophage migration inhibitory factor in acute kidney injury after cardiac surgery. *Sci Transl Med*. 2018;10:eaan4886.
48. Vader P, Mol EA, Pasterkamp G, et al. Extracellular vesicles for drug delivery. *Adv Drug Deliv Rev*. 2016;106:148–156.
49. Rufino-Ramos D, Albuquerque PR, Carmona V, et al. Extracellular vesicles: novel promising delivery systems for therapy of brain diseases. *J Control Release*. 2017;262:247–258.
50. Marcus ME, Leonard JN. FedExosomes: engineering therapeutic biological nanoparticles that truly deliver. *Pharmaceuticals*. 2013;6:659–680.
51. Liu M, Ning X, Li R, et al. Signalling pathways involved in hypoxia-induced renal fibrosis. *J Cell Mol Med*. 2017;21:1248–1259.